International Journal of Power Electronics and Drive Systems (IJPEDS)
Vol. 16, No. 1, March 2025, pp. 151~161
ISSN: 2088-8694, DOI: 10.11591/ijpeds.v16.i1.pp151-161

Efficiency enhanced adaptive quasi-sliding mode controller for variable-speed induction motor drive

Shaija Palackappillil Jacob[1], Asha Elizabeth Daniel[2]
[1]Department of Electrical and Electronics Engineering, Govt. Model Engineering College, Kochi, India
[2]Division of Electrical and Electronics Engineering, School of Engineering, CUSAT, Kochi, India

Article Info

Article history:

Received May 21, 2024
Revised Nov 27, 2024
Accepted Dec 9, 2024

Keywords:

Adaptive control
Efficiency enhancement
Induction motor drive
Lookup table
Loss model
Non-linear control
Sliding mode control

ABSTRACT

Recent advancements in automated manufacturing and processing industries necessitate fast-responding, efficient, and robust methods for controlling induction motor (IM) drives. Classical proportional-integral (PI) controllers provide optimal performance only at specific operating points and are sensitive to parameter variations. This work proposes an adaptive quasi-sliding mode controller (AQSMC), which utilizes a tangent (tanh) function as the switching function and demonstrates enhanced robustness and adaptability across a wider range of operating conditions. The AQSMC employs an adaptation law to estimate the dynamic disturbances, offering insensitivity to structured and unstructured uncertainties. Numerical simulations are carried out with the AQSMC that analytically deduces the optimum field flux ensuring efficient performance. A lookup table derived from the efficiency optimization algorithm (EOA) is incorporated to further streamline the computational requirements. To validate simulation results, a prototype was developed using a 1 HP induction motor, a DSP controller board with a TI C2000 Delfino MCU F28379D microcontroller, and an IGBT-based Inverter module. Simulations show a 6.3% efficiency improvement at half load and 300 rpm, while experimental analysis records a 3.9% improvement with the EOA, highlighting the potential for enhancing energy efficiency in various industrial applications.

Corresponding Author:

Shaija Palackappillil Jacob
Department of Electrical and Electronics Engineering, Govt. Model Engineering College
Kochi, Kerala, India
Email: shaijapj@gmail.com, shaija@mec.ac.in

1. INTRODUCTION

Induction motors (IMs) are widely used in industrial applications due to their affordability, rugged construction, high efficiency, and self-starting capabilities. These features make IMs suitable for a wide range of applications that require minimal maintenance and high reliability. However, controlling IMs as variable-speed drives remains a challenging task, mainly due to their complex, multivariable, non-linear behavior, and dynamic fluctuations in electrical characteristics. Advanced control schemes such as field-oriented control (FOC) have been developed to address these complexities. FOC facilitates the decoupling of torque and flux by employing dynamic d-q modeling of the motor in a synchronously rotating reference frame, enabling precise control over motor operation [1], [2].

Classical proportional-integral (PI) controllers offer optimal performance only at specific operating points and are sensitive to parameter variations, making them less effective in dynamic environments. Sliding mode control (SMC) has emerged as a robust, non-linear control method capable of handling the uncertainties and variations inherent in IM drives. By applying a discontinuous control signal, SMC modifies the system's dynamics to guide the state trajectories onto a predefined surface in the state space, ultimately achieving accurate tracking either asymptotically or in finite time [3], [4]. However, conventional SMC is often associated with high-frequency chattering [5] due to the use of switching functions like the signum function, which assumes instantaneous switching. Practical limitations such as control computation delays, sensor inaccuracies, and the dead time of power electronic switches contribute to this chattering phenomenon [6], [7]. High-frequency chattering can be problematic in control systems. It leads to excessive control activity, increased power consumption, and potential damage to components like actuators [8]. Additionally, it introduces unwanted internal non-linearities, leading to instability in certain applications. In the context of induction motors, chattering manifests as current harmonics and torque pulsations, resulting in degraded system performance [9], [10].

The proposed quasi-sliding mode controller (QSMC) addresses this issue by using a continuous control input, approximating the discontinuous signum function with a smooth function, such as the hyperbolic tangent function (tanh), to effectively reduce chattering [11]. In the presence of uncertainties, QSMC confines system states within a predictable and adjustable bound near the origin, ensuring reliable performance even when ideal sliding mode is not achieved [12]. This method has been effectively employed to reduce chattering in various applications, such as DC-DC converter switching [13], motor speed control [6], [14], [15], and electro-hydraulic actuator systems [16]. In spacecraft applications, the use of tanh function instead of the signum function leads to quicker response and lower power consumption for pointing man oeuvres, as reported in the literature [17]. When the upper bound for parameter variations cannot be predicted in practical applications, a high sliding gain is often chosen in SMC design, leading to increased chattering and unnecessary control activity [18]. The proposed adaptive quasi-sliding mode controller (AQSMC) overcomes this by employing an adaptation law to estimate and adjust the sliding gain in real-time, ensuring efficient and robust control without the need to pre-calculate upper bounds.

As global electricity demand continues to rise, driven by industrial growth and improved living standards, enhancing energy efficiency in all engineering domains becomes imperative [19]. Remarkably, electric motors, particularly induction motors, consume over half of the world's total electricity [20]. While IMs operate most efficiently near their rated conditions, they often function far from their rated capacity in many real-world applications, such as elevators running at less than half their rated torque [21]. This inefficiency not only impacts operational performance but also increases energy costs and environmental impact. Therefore, optimizing control strategies for IMs in varying load conditions is essential. Electric vehicles, for example, can benefit significantly from energy-efficient control strategies, thereby extending battery life and vehicle range [22]. A substantial portion of losses in IMs, approximately 70%, can be attributed to copper and iron losses, which are influenced by the motor's electrical and magnetic loading [21]. Maintaining rated flux under partial load conditions results in higher magnetic losses compared to electrical losses. FOC-based IM drives have demonstrated significant energy savings at partial loads and various speeds when controllers operate at the minimum loss point [23], leading to efficiency improvements, especially in applications with non-linear torque-speed characteristics, such as fans or pumps [24].

To enhance machine efficiency, especially in light-load situations, various techniques have been proposed for IM drives. These efficiency optimization control (EOC) techniques differ in approach, complexity, accuracy, and convergence [25]. The literature broadly classifies EOC techniques into three categories: loss model-based control (LMC), search control (SC), and hybrid control (HC) [26]. LMC involves adjusting the magnetization level analytically by considering a specific machine model [19], [27], reducing power losses based on criteria such as flux, slip speed, power factor, or the d-axis component of the stator current [28]–[31]. The SC technique iteratively modifies the magnetization level to find the minimum input power but may suffer from slow convergence and objectionable torque dynamics [23], [32], [33]. To further enhance the efficiency of induction motors (IMs), various search techniques utilizing nature-inspired algorithms and neural networks (NNs) have been reported, yielding promising results in identifying optimal control parameters for improved performance and energy savings [34]–[37].

The key contributions of this paper include the development and implementation of an adaptive, efficiency-enhanced variable-speed controller with a hyperbolic tangent switching function. The efficiency optimization algorithm (EOA) based on a loss model is designed to deduce the optimal d-axis stator current in real-time for varying speed and load conditions. The proposed AQSMC effectively reduces chattering and enhances control performance. Extensive simulations carried out in MATLAB/Simulink and experimental validation underscore the robustness and practicality of the proposed control strategy. The approach is established as a viable solution for enhancing induction motor drive efficiency while providing robust control across varying load and speed conditions in different applications.

The adaptive quasi-sliding mode speed controller design based on equivalent control technique is included in section 2 and efficiency optimization algorithm design based on IM loss model in section 3. Section

4 covers the simulation results and section 5 experimental analysis. Conclusion and future scope are included in section 6.

2. ADAPTIVE QUASI-SLIDING MODE CONTROLLER (AQSMC)

In this section, an adaptive quasi-sliding mode controller is designed for controlling the speed of the induction motor. In this method, a QSMC is designed with a continuous hyperbolic tangent (tanh) function in place of the discontinuous signum function of conventional SMC in anticipation of a better response and chattering reduction. An equivalent control technique is applied in which the control signal u_c can be written as (1) [38].

$$u_c = u_{eq} + u_n \tag{1}$$

Where, u_{eq} is the equivalent control signal, ensuring system convergence, and u_n is the switching control signal, ensuring that the sliding surface is drawn to the system state space. The sliding plane S is defined as a function of the speed error e(t) and its integral and is given by (2).

$$S = K_1 . e + K_2 \int e . dt \tag{2}$$

The derivative of the Lyapunov energy function is negative definite, which guarantees the state trajectory's motion to the sliding surface. i.e. as in (3).

$$\dot{S}_{(t)} . S_{(t)} < 0 \tag{3}$$

The switching control component is given by (4).

$$u_n = \zeta_m \tanh\left(\frac{S}{\epsilon}\right) \tag{4}$$

Where, the switching gain, ζ_m, is the output saturation value of the controller, and its value is set to meet the uncertainties of the system. The tanh function is a rescaled logistic sigmoid function given by (5) [39].

$$\tanh\left(\frac{S}{\epsilon}\right) = \frac{e^{\left(\frac{S}{\epsilon}\right)} - e^{-\left(\frac{S}{\epsilon}\right)}}{e^{\left(\frac{S}{\epsilon}\right)} + e^{-\left(\frac{S}{\epsilon}\right)}} \tag{5}$$

Where, S is the sliding variable and ϵ is the boundary layer width which determines the steepness or inclination of the tanh function (ϵ>0). The steepness of the tanh function determines how closely the tanh function can resemble the signum function.

Prior knowledge of the upper bound of the parameter variations, unmodeled dynamics, and noise magnitudes, is required to decide the value of switching gain [40]. This upper bound should be determined as precisely as possible because the higher the upper bound, the higher should be the switching gain [41]. A suitably high value for the switching gain is usually used as this upper bound is challenging to calculate. However, this could result in a control signal that is too high or more control activity than is necessary to achieve the control objective [18]. This is undesirable in IM control as it implies higher i_{qs_ref} and increases the chattering phenomenon. The proposed AQSMC scheme continuously estimates the sliding gain to adapt to evolving system uncertainties over time.

The switching gain $\hat{\zeta}$ is estimated as per the following adaptation law, as in (6).

$$\dot{\hat{\zeta}} = \gamma \, |S| \tag{6}$$

Where, γ is a positive constant that determines the switching gain's adaptation speed and $\hat{\zeta}_{(0)} = 0$. The high control activity in the reaching phase can be effectively avoided by selecting an appropriate adaptation gain. The modified switching control component is given by (7).

$$u_n = \hat{\zeta} \, \gamma \, \tanh\left(\frac{S}{\epsilon}\right) \tag{7}$$

There exists an unknown finite non-negative switching gain ζ such that in (8).

$$\zeta > L_{max} + \eta \quad (8)$$

Where, η is a positive constant and $L_{max} \geq |L_{(t)}| \; \forall \, t$. The uncertainty terms have been collected in the signal L(t) [38]. The tracking error exponentially approaches zero when sliding mode occurs on the sliding surface, S(t) = $\dot{S}$(t) = 0 [41]. By using the gain adaptation law, the obtained control magnitude is reasonable, as the gain-adaptation law does not overestimate the magnitude of uncertainties or perturbations.

3. EFFICIENCY OPTIMIZATION ALGORITHM (EOA) BASED ON LOSS-MODEL OF IM

The percentage efficiency of the IM drive system is investigated using both the conventional PI controller and the proposed AQSMC under varying load conditions. Although the adaptive controller exhibits substantial improvement in transient performance compared to the PI controller, the efficiency across various loads shows a slight downgrade trend. Therefore, there is potential for efficiency optimization to further enhance overall controller performance. This section introduces an EOA designed to minimize total losses in the IM at all operating conditions. The losses in an IM include copper losses P_{cu}, core losses or iron losses P_{fe} and mechanical losses P_{mech}. The copper losses occur in a machine due to current flow through stator and rotor windings. Under steady-state, the total copper losses are computed as (9) [42].

$$P_{cu} = \frac{3}{2} R_s \left({i_{ds}}^2 + {i_{qs}}^2 \right) + \frac{3}{2} R_r \left({i_{dr}}^2 + {i_{qr}}^2 \right) \quad (9)$$

Where, Rs denotes the stator resistance and R_r, rotor resistance. The d-axis and q-axis components of stator and rotor currents are given by i_{ds}, i_{qs}, i_{dr} and i_{qr} respectively. The core losses consist of eddy current losses and hysteresis losses.

$$P_{fe} = \frac{3}{2} \left(k_h \omega_e + k_e {\omega_e}^2 \right) {\Psi_m}^2 \quad (10)$$

Where, k_h denotes the hysteresis loss coefficient and k_e is the eddy current loss coefficient. Synchronous speed is given by ω_e and mutual flux is denoted by Ψ_m. Mechanical losses include friction due to bearing and windage losses. Mechanical losses, as an approximation, are proportional to the square of the rotor speed.

$$P_{mech} = k_m {\omega_r}^2 \quad (11)$$

Where, k_m is the mechanical loss coefficient and ω_r is the rotor mechanical speed. Hence, the total power losses in the IM can be expressed as (12).

$$P_{loss} = \frac{3}{2} \left\{ R_s \left({i_{ds}}^2 + {i_{qs}}^2 \right) + R_r \left({i_{dr}}^2 + {i_{qr}}^2 \right) + \left(k_h \omega_e + k_e {\omega_e}^2 \right) {\Psi_m}^2 \right\} + k_m {\omega_r}^2 \quad (12)$$

When the motor is running under steady-state and in the rotor field-oriented control [28].

$$i_{dr} = 0; \text{ and } i_{qr} = -\frac{L_m}{L_r} i_{qs} \quad (13)$$

Where L_m is the mutual inductance and L_r rotor inductance. Here, the air-gap flux can be derived as (14) and (15) [43].

$${\Psi_m}^2 = (L_m i_{ds})^2 + \left(L_m i_{qs} - \frac{{L_m}^2}{L_r} i_{qs} \right)^2 \quad (14)$$

$${\Psi_m}^2 = {L_m}^2 {i_{ds}}^2 + \frac{{L_m}^2 {L_{lr}}^2}{{L_r}^2} {i_{qs}}^2 \quad (15)$$

Where, $L_r = L_{lr} + L_m$. Also, the motor Torque developed in IFOC is given by (16).

$$T_e = \frac{3}{2} \frac{P}{2} \frac{{L_m}^2}{L_r} i_{qs} i_{ds} = K_t i_{qs} i_{ds} \quad (16)$$

From the (16), i_{qs} can be written as (17).

$$i_{qs} = \frac{T_e}{K_t\, i_{ds}} \tag{17}$$

Where $K_t = \frac{3}{2}\frac{P}{2}\frac{L_m{}^2}{L_r}$. Using in (13) and (15), (12) can be written as (18).

$$P_{loss} = \frac{3}{2}\left\{\begin{matrix}\left(R_s + (k_h\omega_e + k_e\omega_e{}^2)\, L_m{}^2\right).\, i_{ds}{}^2 + \\ \left(R_s + R_r\frac{L_m{}^2}{L_r{}^2} + (k_h\omega_e + k_e\omega_e{}^2)\frac{L_{lr}{}^2 L_m{}^2}{L_r{}^2}\right).\, i_{qs}{}^2\end{matrix}\right\} + k_m\omega_r{}^2 \tag{18}$$

Substituting (17) in (18), it becomes (19).

$$P_{loss} = \frac{3}{2}\left(K_a.\, i_{ds}{}^2 + K_b.\frac{T_e{}^2}{K_t{}^2\, i_{ds}{}^2}\right) + k_m\omega_r{}^2 \tag{19}$$

Where, $K_a = R_s + (k_h\omega_e + k_e\omega_e{}^2)\, L_m{}^2$; and $K_b = R_s + R_r\frac{L_m{}^2}{L_r{}^2} + (k_h\omega_e + k_e\omega_e{}^2)\frac{L_{lr}{}^2 L_m{}^2}{L_r{}^2}$.

The loss (19) expresses the induction motor losses in terms of i_{ds}. That is, the loss expression is dependent on the d-axis stator current component, i_{ds} , at each operating point (corresponding to ω_r and T_L), presuming that the motor parameters are fixed and not dependent on rotor flux. The optimal value of the d-axis stator current i_{ds} that minimizes the overall power loss is computed by differentiating the (19) with respect to i_{ds} and equating it to zero as (20) and (21):

$$\frac{dP_{loss}}{di_{ds}} = \frac{3}{2}\left(2.\, K_a.\, i_{ds} - \left(\frac{T_e}{K_t}\right)^2\frac{2.K_b}{i_{ds}{}^3}\right) = 0 \tag{20}$$

$$\text{and } i_{ds_{opt}} = \sqrt[4]{\frac{K_b}{K_a}\left(\frac{T_e}{K_t}\right)^2} \tag{21}$$

So, in this control technique, an EOA is presented that computes the optimum value of the primary control variable, the d-axis component of stator current, i_{ds}, which in turn minimizes the losses and maximizes the efficiency.

4. SIMULATION RESULTS AND DISCUSSION

The proposed EOA is developed with the loss model of the IM in MATLAB/Simulink for a 1 HP IM drive. The algorithm will deduce the optimal value of the d-axis stator current (i_{ds}) in real time, depending on the speed/load conditions. Machine parameters for the 1HP IM drive are listed in Table 1. The nominal value of flux in d-axis is taken as 0.8. The AQSMC proposed in section 2 is used as the speed controller in indirect FOC scheme as shown in Figure 1.

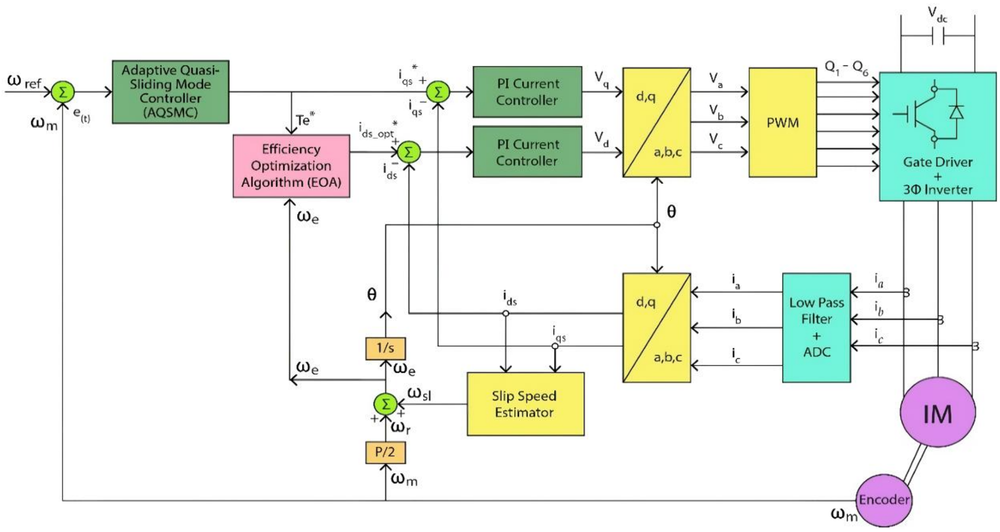

Figure 1. Block schematic of the proposed efficiency-optimized IM drive

Table 1. Parameters of 1 HP induction motor

Parameter	Value
Rated power	750 W
No. of phases	3
Rs	10 Ω
Rr	5.64 Ω
Rc	1273 Ω
Lls	0.0386H
Llr	0.0386H
Lm	0.5353H
Rated torque	5.1 Nm
J	0.008 kg m^2
B	0.000503 kg m^2/s
Poles	4
Rated speed	1380 rpm
Rated voltage	415 $V_{(L-L)}$

4.1. Optimal I_{ds}

The optimal values of i_{ds} corresponding to each speed/output load condition are found out using EOA and is plotted in Figure 2. At a fixed load torque, say T_{fl}, if speed is varied from 1400 rpm to 300 rpm, the optimal i_{ds} value varies as shown in Figure 2. Optimal value of i_{ds} goes on decreasing as load torque is decreased corresponding to all speed conditions, as observed from Figure 2.

4.2. Reduction in Ploss

The reduction in power loss by using optimal i_{ds} compared to fixed i_{ds} is illustrated in Figure 3. The most significant reduction occurs under heavy load and low-speed conditions with the optimal i_{ds}. A maximum reduction of 116 W in power loss is observed in the simulation for the 1 Hp IM drive. A maximum power loss reduction of 116 W is observed in the simulation for the 1 HP IM drive. Each graph corresponds to a specific load torque condition with speed variation, and all exhibit a consistent trend.

4.3. Efficiency enhancement

Simulations are carried out for all possible speed/load conditions, and power input and efficiency are noted with fixed i_{ds} control and optimal i_{ds} control using EOA. The efficiency of the system obtained with fixed i_{ds} value for different speed/load torque conditions are tabulated in Table 2 and that corresponding to optimal i_{ds} using EOA are given in Table 3.

The efficiency of the drive system with and without EOA algorithm are found out in simulation and the curves are plotted with respect to output power in Figure 4. Each curve corresponds to a speed condition with varying loads. A maximum of 27.57% improvement in efficiency is observed in the simulation at 300 rpm, full load torque.

4.4. Lookup table-based efficiency optimization control

A lookup table is also developed using the optimal i_{ds} values derived from the simulated results of the EOA algorithm for all operating speed/load conditions. In this approach, the optimal value of i_{ds} is retrieved from this lookup table, eliminating the need for analytical deduction using the EOA algorithm. This not only streamlines the process but also reduces computational complexity. The lookup table containing the optimal i_{ds} values is presented in Table 4.

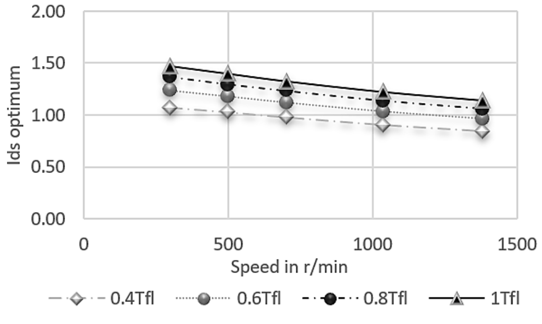

Figure 2. Optimal values of i_{ds} for different speed/load conditions

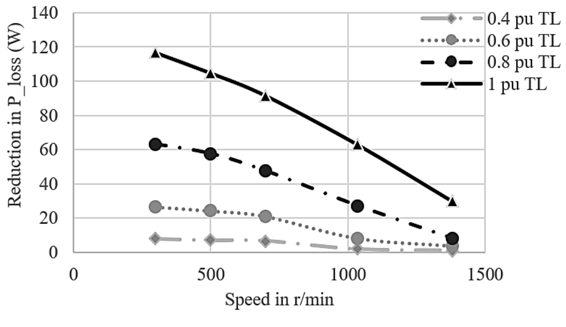

Figure 3. Reduction in P_{loss} for different speed/load conditions

Table 2. Efficiency of AQSMC IM drive with fixed i_{ds}

Torque	Speed (rpm)				
	300	500	700	1035	1380
0.1Tfl	22.37	28.63	33.88	38.68	42.48
0.2Tfl	33.1	41.97	47.25	53.01	56.38
0.3Tfl	38.02	47.4	53.52	59.79	63.05
0.4Tfl	39.48	50.15	56.37	63.02	66.81
0.5Tfl	39.65	50.52	56.98	64.11	68.7
0.6Tfl	38.83	49.93	57.01	64.8	69.47
0.7Tfl	37.49	49.01	56.62	64.51	69.68
0.8Tfl	36.09	47.64	55.37	64.06	69.67
0.9Tfl	34.68	46.38	54.39	63.38	69.38
1.0Tfl	33.51	45.18	53.24	62.57	68.84

Table 3. Efficiency of AQSMC IM drive with EOA (optimal i_{ds})

Torque	Speed (rpm)				
	300	500	700	1035	1380
0.1Tfl	26.71	33.92	39.82	44.06	46.4
0.2Tfl	35.29	44.14	50.53	55.57	57.94
0.3Tfl	39.37	49.66	55.24	60.31	63.42
0.4Tfl	41.53	51.72	57.82	63.19	66.84
0.5Tfl	42.05	53.28	59.03	64.85	68.76
0.6Tfl	43.45	53.9	60.25	65.76	69.53
0.7Tfl	43.8	54.21	60.66	66.52	69.74
0.8Tfl	43.7	54.6	60.61	66.52	70.3
0.9Tfl	43.75	54.91	61.05	67.05	70.59
1.0Tfl	42.75	54.71	61.13	67.3	70.75

Table 4. Lookup table for optimal i_{ds}

Torque (pu)	Speed (rpm)				
	300	500	700	1035	1380
0.1Tfl	0.68	0.65	0.62	0.58	0.55
0.2Tfl	0.85	0.82	0.78	0.72	0.68
0.3Tfl	0.98	0.93	0.89	0.83	0.77
0.4Tfl	1.07	1.03	0.98	0.91	0.85
0.5Tfl	1.16	1.11	1.05	0.97	0.91
0.6Tfl	1.23	1.18	1.12	1.03	0.97
0.7Tfl	1.30	1.24	1.18	1.09	1.02
0.8Tfl	1.37	1.29	1.23	1.14	1.06
0.9Tfl	1.42	1.35	1.28	1.18	1.10
1.0Tfl	1.47	1.40	1.32	1.22	1.14

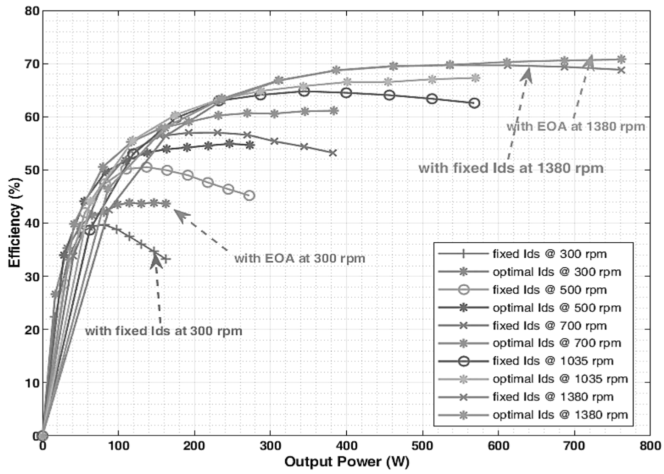

Figure 4. Efficiency curves for fixed-speed, varying-load with and without EOA

5. EXPERIMENTAL RESULTS AND AND DISCUSSION

A prototype has been built with a 1 HP induction motor, a DSP controller board using a TI C2000 Delfino MCU F28379D microcontroller, and an IGBT-based IPM Inverter module to validate simulation results, the photograph of which is shown in Figure 5. The motor speed is sensed by a 2-phase incremental type optical rotary encoder with 600 pulses per revolution, which offers high resolution, excellent accuracy, and quick response times. The encoder's quadrature output facilitates precise position and speed measurements, making it ideal for applications requiring fine control. Additionally, low-pass filtering circuitry is employed in the current sensors to minimize high-frequency noise, ensuring that the integrity of the measurements is preserved. The speed of the IM drive is controlled experimentally using the AQSM controller. The performance parameters of these controllers are analyzed in simulation and are experimentally validated.

5.1. Efficiency enhancement

The developed IM drive with AQSM controller is run at half load and 300 rpm, and the corresponding efficiency of the drive is measured. The overall system efficiency is 39.6% in simulation and 38% in experimentation. The TI microcontroller is again loaded with the drive model incorporating the EOA, which provides the optimal i_{ds} value, and is run under identical speed and load conditions. Efficiency with the EOA improves to 42.1% in simulation and 39.5% in experiment. The hardware drive efficiency with fixed i_{ds} closely matches the simulated results, within a tolerance limit of 4.2%, while with the EOA, the system efficiency in hardware remains within a tolerance limit of 6.6% of the simulated outcome. For an input speed of 300 rpm at half-rated load, the optimal i_{ds} provides a 6.3% efficiency improvement in simulation and a 3.9% in experimental analysis. The close agreement between the simulated and the experimental results confirms the validity of the proposed technique.

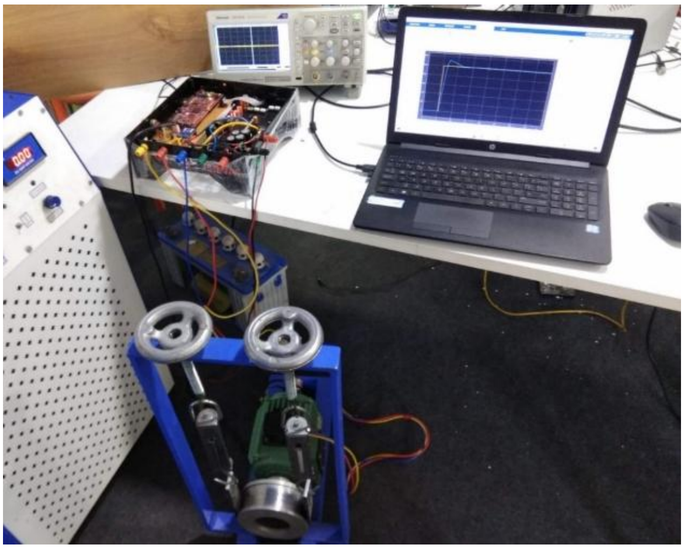

Figure 5. Hardware setup of the developed IM drive

5.2. Speed response

The speed response of the AQSM controller with fixed i_{ds} under simulation and experimental analysis are presented in Figure 6 and its transient analysis in Figure 7, respectively. The speed response of the AQSM controller with optimal i_{ds} under simulation and experimental analysis are presented in Figure 8. and its transient analysis in Figure 9, respectively. While comparing Figures 7 and 9, it can be concluded that by incorporating the EOA algorithm not only improves the efficiency but also reduces the settling time, peak time and peak overshoot in practical implementation.

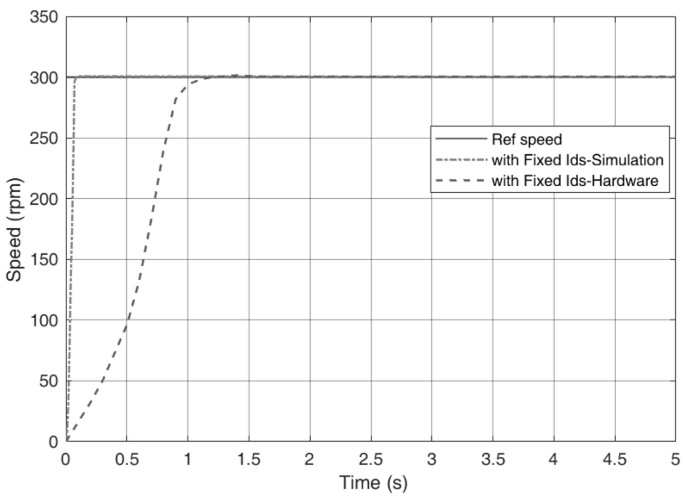

Figure 6. Speed response of the AQSM controller with fixed i_{ds} in simulation and in hardware

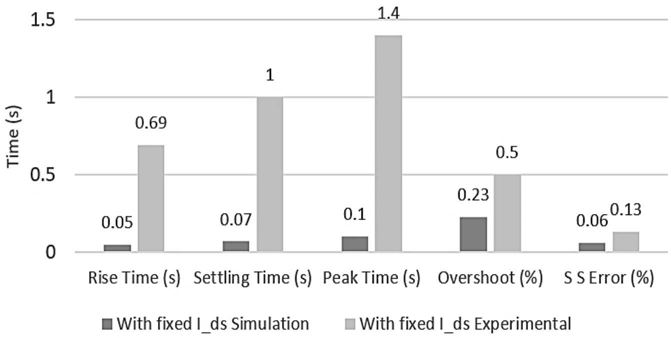

Figure 7. Transient analysis of AQSMC with fixed i_{ds} in simulation and in hardware

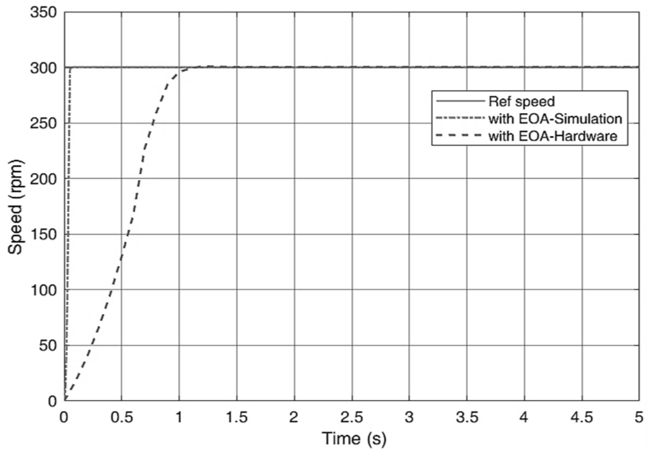

Figure 8. Speed response of the AQSM controller with optimal i_{ds} in simulation and in hardware

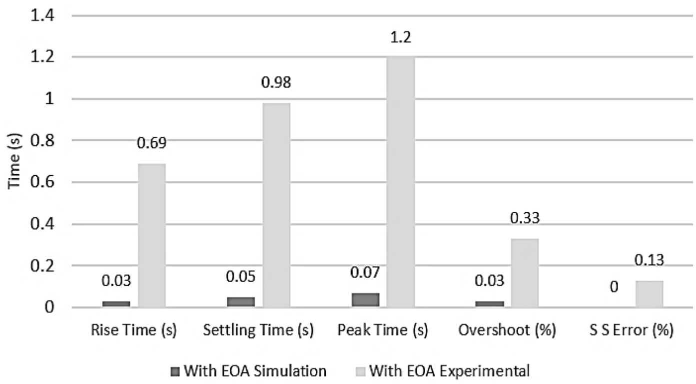

Figure 9. Transient analysis of AQSMC with EOA in simulation and in hardware

6. CONCLUSION

This paper proposes an adaptive, efficiency-enhanced, variable-speed non-linear controller for optimal speed control of IM drives, featuring reduced computational complexity. An adaptive quasi-sliding mode controller is designed using a tan function as the switching function, along with an integral control law that adheres to the Lyapunov stability condition. The AQSMC offers robust control performance by effectively managing system uncertainties and non-linearities while ensuring stability and minimizing chattering through the real-time adaptation of the sliding gain. To enhance efficiency, an efficiency optimization algorithm (EOA) based on a loss model is incorporated that will dynamically search for the optimal d-axis current in real time across all load and speed conditions. Extensive MATLAB simulations demonstrate that the EOA effectively identifies optimal i_{ds} values, which are stored in a lookup table for efficient implementation.

The AQSM controller, combined with the EOA, is successfully implemented on a TI F28379D DSP controller for a 1 HP IM drive. Results indicate a significant efficiency improvement of 6.3% in simulation and 3.9% in experimental analysis at half load and 300 rpm compared to the system without the EOA. The hardware efficiency with fixed i_{ds} closely matches the simulation results, maintaining a tolerance of 4.2%. Additionally, with the EOA, the system efficiency in hardware is within a tolerance of 6.5% of the simulated results. These findings validate the proposed method's effectiveness in enhancing IM drive efficiency. Future work can explore extending this approach to higher-rated motors and incorporating hybrid control techniques to further enhance efficiency across diverse industrial applications, including electric vehicles and renewable energy systems, ultimately optimizing motor performance and sustainability.

REFERENCES

[1] B. K. Bose, "Modern Power Electronics and AC Drives," *Prentice-Hall*, p. 738, 2002, [Online]. Available: http://scholar.google.com/scholar?hl=en&btnG=Search&q=intitle:Modern+Power+Electronics+and+AC+drives#0

[2] J. Iqbal, M. Ullah, S. G. Khan, B. Khelifa, and S. Ćuković, "Nonlinear control systems - A brief overview of historical and recent advances," *Nonlinear Engineering*, vol. 6, no. 4, pp. 301–312, 2017, doi: 10.1515/nleng-2016-0077.

[3] J. Liu, "Sliding mode control using MATLAB," *Sliding Mode Control Using MATLAB*, pp. 1–332, 2017.

[4] J. Slotine and W. Li, "Applied Nonlinear Control," 1991. [Online]. Available: http://scholar.google.com/scholar?hl=en&btnG=Search&q=intitle:Slotine+?+Li+APPLIED+NONLINEAR+CONTROL+!#1

[5] L. Wu, J. Liu, S. Vazquez, and S. K. Mazumder, "Sliding Mode Control in Power Converters and Drives: A Review," *IEEE/CAA Journal of Automatica Sinica*, vol. 9, no. 3, pp. 392–406, 2022, doi: 10.1109/JAS.2021.1004380.

[6] M. S. Zaky, "Robust chatter-free continuous VSC for the speed control of electrical motor drives using adaptive feedback gain," *Electric Power Systems Research*, vol. 140, pp. 786–796, 2016, doi: 10.1016/j.epsr.2016.05.007.

[7] K. Makhloufi, I. K. Bousserhane, and S. A. Zegnoun, "Adaptive fuzzy sliding mode controller design for pmlsm position control," *International Journal of Power Electronics and Drive Systems*, vol. 12, no. 2, pp. 674–684, 2021, doi: 10.11591/ijpeds.v12.i2.pp674-684.

[8] T. D. Chuyen *et al.*, "Improving control quality of PMSM drive systems based on adaptive fuzzy sliding control method," 2022. doi: 10.11591/ijpeds.v13.i2.pp835-845.

[9] A. Saghafinia, H. W. Ping, M. N. Uddin, and K. S. Gaeid, "Adaptive fuzzy sliding-mode control into chattering-free im drive," *IEEE Transactions on Industry Applications*, vol. 51, no. 1, pp. 692–701, 2015, doi: 10.1109/TIA.2014.2328711.

[10] P. J. Shaija and A. E. Daniel, "Robust Sliding Mode Control Strategy Applied to IFOC Induction Motor Drive," in *2021 4th International Conference on Electrical, Computer and Communication Technologies, ICECCT 2021*, 2021, doi: 10.1109/ICECCT52121.2021.9616948.

[11] Y. Shtessel, C. Edwards, L. Fridman, and A. Levant, *Sliding Mode Control and Observation*, vol. 10. in Control Engineering, vol. 10. New York, NY: Springer New York, 2014. doi: 10.1007/978-0-8176-4893-0.

[12] C. F. Huang, J. S. Lin, T. L. Liao, C. Y. Chen, and J. J. Yan, "Quasi-sliding mode control of chaos in permanent magnet synchronous motor," *Mathematical Problems in Engineering*, vol. 2011, 2011, doi: 10.1155/2011/964240.

[13] K. B. Siddesh, B. Banakara, and R. Shivarudraswamy, "Enhanced sliding mode controller performance in DC-DC buck converter using a tan hyperbolic reaching law and constant plus proportional reaching law," *Bulletin of Electrical Engineering and Informatics*, vol. 9, no. 2, pp. 525–532, 2020, doi: 10.11591/eei.v9i2.2100.

[14] P. J. Shaija and A. E. Daniel, "Parameter Tuning of Sliding Mode Speed Controller of Induction Motor Drive Using Teaching-Learning Based Optimization Algorithm," *International Review of Automatic Control*, vol. 15, no. 1, pp. 28–37, 2022, doi: 10.15866/ireaco.v15i1.21953.

[15] J. R. B. A. Monteiro, C. M. R. Oliveira, and M. L. Aguiar, "Sliding mode control of brushless DC motor speed with chattering reduction," *IEEE International Symposium on Industrial Electronics*, vol. 2015-September, pp. 542–547, 2015, doi: 10.1109/ISIE.2015.7281525.

[16] C. C. Soon, R. Ghazali, M. F. Ghani, C. M. Shern, Y. M. Sam, and Z. Has, "Chattering Analysis of an Optimized Sliding Mode Controller for an Electro-Hydraulic Actuator System," *Journal of Robotics and Control (JRC)*, vol. 3, no. 2, pp. 160–165, 2022, doi: 10.18196/jrc.v3i2.13671.

[17] M. Mancini, E. Capello, and E. Punta, "Sliding mode control with chattering attenuation and hardware constraints in spacecraft applications," *IFAC-PapersOnLine*, vol. 53, no. 2, pp. 5147–5152, 2020, doi: 10.1016/j.ifacol.2020.12.1174.

[18] O. Barambones and P. Alkorta, "A robust vector control for induction motor drives with an adaptive sliding-mode control law," *Journal of the Franklin Institute*, vol. 348, no. 2, pp. 300–314, 2011, doi: 10.1016/j.jfranklin.2010.11.008.

[19] P. K. Choudhary and U. K. Choudhary, "Efficiency optimization of pump motor drive at steady-state condition," in *IEEE International Conference on Power, Control, Signals and Instrumentation Engineering, ICPCSI 2017*, 2018, pp. 342–347, doi: 10.1109/ICPCSI.2017.8392312.

[20] A. M. Bazzi and P. T. Krein, "Review of methods for real-time loss minimization in induction machines," *IEEE Transactions on Industry Applications*, vol. 46, no. 6, pp. 2319–2328, 2010, doi: 10.1109/TIA.2010.2070475.

[21] P. K. Choudhary, S. P. Dubey, B. Tiwari, and B. Dewangan, "Efficiency optimization of induction motor drive using Artificial Neural Network," in *2016 International Conference on Energy Efficient Technologies for Sustainability, ICEETS 2016*, 2016, pp. 821–827, doi: 10.1109/ICEETS.2016.7583860.

[22] P. Melo, R. de, and R. Esteves, "Evaluation of an Energy Loss-Minimization Algorithm for EVs Based on Induction Motor," *Induction Motors - Modelling and Control*, 2012, doi: 10.5772/52280.

[23] D. S. Kirschen, D. W. Novotny, and T. A. Lipo, "Optimal Efficiency Control of an Induction Motor Drive," *IEEE Transactions on Energy Conversion*, vol. EC-2, no. 1, pp. 70–76, Mar. 1987, doi: 10.1109/TEC.1987.4765806.

[24] P. Famouri and J. J. Cathey, "Loss minimization control of an induction motor drive," *IEEE Transactions on Industry Applications*, vol. 27, no. 1, pp. 32–37, 1991, doi: 10.1109/28.67529.

[25] C. M. Ta and Y. Hori, "Convergence improvement of efficiency-optimization control of induction motor drives," *IEEE Transactions on Industry Applications*, vol. 37, no. 6, pp. 1746–1753, 2001, doi: 10.1109/28.968187.

[26] A. Bruno, M. Caruso, A. O. DI Tommaso, R. Miceli, C. Nevoloso, and F. Viola, "Simple and Flexible Power Loss Minimizer with Low-Cost MCU Implementation for High-Efficiency Three-Phase Induction Motor Drives," *IEEE Transactions on Industry Applications*, vol. 57, no. 2, pp. 1472–1481, 2021, doi: 10.1109/TIA.2021.3051581.

[27] M. Sreejeth, M. Singh, and P. Kumar, "Efficiency enhancement for indirect vector-controlled induction motor drive," *International Journal of Electronics*, vol. 106, no. 9, pp. 1281–1294, 2019, doi: 10.1080/00207217.2019.1584921.

[28] F. C. Lin and S. M. Yang, "On-line tuning of an efficiency-optimized vector controlled induction motor drive," *Tamkang Journal of Science and Engineering*, vol. 6, no. 2, pp. 103–110, 2003.

[29] A. S. Kosmodamianskii, V. I. Vorob'Ev, and A. A. Pugachev, "Induction motor drives with minimal power losses," *Russian Electrical Engineering*, vol. 83, no. 12, pp. 667–671, 2012, doi: 10.3103/S1068371212120073.

[30] D. Hu, W. Xu, R. Dian, Y. Liu, and J. Zhu, "Loss Minimization Control of Linear Induction Motor Drive for Linear Metros," *IEEE Transactions on Industrial Electronics*, vol. 65, no. 9, pp. 6870–6880, 2018, doi: 10.1109/TIE.2017.2784343.

[31] M. N. Uddin and S. W. Nam, "New online loss-minimization-based control of an induction motor drive," *IEEE Transactions on Power Electronics*, vol. 23, no. 2, pp. 926–933, 2008, doi: 10.1109/TPEL.2007.915029.

[32] M. Caruso, A. O. Di Tommaso, R. Miceli, C. Spataro, and F. Viola, "Experimental investigation on high-efficiency control algorithms for three-phase induction motors," in *24th IMEKO TC4 International Symposium and 22nd International Workshop on ADC and DAC Modelling and Testing*, 2020, pp. 479–484,

[33] G. Khoury, R. Ghosn, F. Khatounian, M. Fadel, and M. Tientcheu, "Energy-efficient field-oriented control for induction motors taking core losses into account," *Electrical Engineering*, vol. 104, no. 2, pp. 529–538, 2022, doi: 10.1007/s00202-021-01321-6.

[34] A. Sharma, R. Gupta, and L. Srivastava, "Implementation of neural network in energy saving of induction motor drives with indirect vector control," *Journal of Theoritical and Applied …*, pp. 774–779, 2008, [Online]. Available: http://citeseerx.ist.psu.edu/viewdoc/download?doi=10.1.1.208.5317&rep=rep1&type=pdf

[35] E. Poirier, M. Ghribi, and A. Kaddouri, "Loss minimization control of induction motor drives based on genetic algorithms," in *IEMDC 2001 - IEEE International Electric Machines and Drives Conference*, 2001, pp. 475–478, doi: 10.1109/IEMDC.2001.939348.

[36] C. T. Raj, S. P. Srivastava, and P. Agarwal, "Energy Efficient Control of Three-Phase Induction Motor - A Review," *International Journal of Computer and Electrical Engineering*, pp. 61–70, 2009, doi: 10.7763/ijcee.2009.v1.10.

[37] S. D. Ho, P. Brandstetter, C. T. Dinh, T. C. Tran, M. C. H. Nguyen, and B. H. Dinh, "On-Line Efficiency-Optimization Control of Induction Motor Drives Using Particle Swarm Optimization Algorithm," 2020, pp. 261–271. doi: 10.1007/978-3-030-14907-9_26.

[38] S. Palackappillil and A. E. Daniel, "Switching function parameter variation analysis of a quasi-sliding mode controlled induction motor drive," *International Journal of Power Electronics and Drive Systems*, vol. 13, no. 2, pp. 733–743, 2022, doi: 10.11591/ijpeds.v13.i2.pp733-743.

[39] P. J. Shaija and A. E. Daniel, "Disturbance Rejection Analysis of a Robust Vector Controlled Induction Motor Drive with an Adaptive Quasi-Sliding Mode Controller," *International Journal on Electrical Engineering and Informatics*, vol. 14, no. 3, pp. 644–661, 2022, doi: 10.15676/ijeei.2022.14.3.10.

[40] A. Pisano, M. Tanelli, and A. Ferrara, "Switched/time-based adaptation for second-order sliding mode control," *Automatica*, vol. 64, pp. 126–132, 2016, doi: 10.1016/j.automatica.2015.11.006.

[41] F. A. Patakor, M. Sulaiman, and Z. Ibrahim, "Adaptive sliding mode for indirect field oriented controlled of induction motor," in *Proceedings - 2011 IEEE Student Conference on Research and Development, SCOReD 2011*, 2011, pp. 289–293, doi: 10.1109/SCOReD.2011.6148752.

[42] J. Li, L. Xu, and Z. Zhang, "A new efficiency optimization method on vector control of induction motors," in *2005 IEEE International Conference on Electric Machines and Drives*, 2005, pp. 1995–2001, doi: 10.1109/iemdc.2005.195993.

[43] M. Sreejeth, M. Singh, and P. Kumar, "Efficiency optimization of vector controlled induction motor drive," in *IECON Proceedings (Industrial Electronics Conference)*, 2012, pp. 1758–1763, doi: 10.1109/IECON.2012.6388935.

BIOGRAPHIES OF AUTHORS

Shaija Palackappillil Jacob received her B.Tech. in Electrical and Electronics Engineering from Mahatma Gandhi University, Kerala, India in 1996 and M.Tech. degree in Opto Electronics and Laser Technology from International School of Photonics, Cochin University of Science and Technology (CUSAT), Kerala, India in 2007. She received her doctoral degree in Electrical Engineering from CUSAT in 2023. She is working as an assistant professor in the Department of Electrical and Electronics Engineering, Govt. Model Engineering College, Kochi, India. Her research interests include the field of power electronics, motor drives, intelligent control, optimization algorithms, and power systems. She can be contacted at email: shaijapj@gmail.com or shaija@mec.ac.in.

Prof. Asha Elizebeth Daniel is a faculty in the Division of Electrical Engineering at Cochin University of Science and Technology, Kerala, India. She has obtained her B.Tech. Degree in Electrical Engineering from NIT Calicut in 1986 and has received her master's and doctoral degrees from IIT Mumbai in 1995 and 2006 respectively. She is currently the Academic Committee Nodal Officer for TEQIP III and the NBA coordinator of the department. She has more than 40 publications to her credit in reputed international journals and international conferences. She can be contacted at email: ashapalal@gmail.com.